

Supplementary Information

Enantiomeric resolution and X-ray optical activity of a tricobalt extended metal atom chain

Anandi Srinivasan,^{†[a,b]} Miguel Cortijo,^{† [a,b,c,d]} Vladimir Bulicanu,^[a,b] Ahmad Naim,^[c,d] Rodolphe Clérac,^[a,b] Philippe Sainctavit,^{*[e]} Andrei Rogalev,^[f] Fabrice Wilhelm,^[f] Patrick Rosa,^[c,d] Elizabeth A. Hillard^{*[a,b]}

Table of Contents

X-ray diffraction

Table S1. Bond lengths [\AA] and angles [$^\circ$] for $\Delta\text{-2}$.	2
Table S2. Bond lengths [\AA] and angles [$^\circ$] for $\Lambda\text{-2}$.	3
Table S3. Bond lengths [\AA] and angles [$^\circ$] for <i>rac</i> -3.	4
Fig. S1. Thermal ellipsoid diagram of the main molecular species in $\Delta\text{-2}$.	5
Fig. S2. Thermal ellipsoid diagram of the main molecular species in $\Lambda\text{-2}$.	5
Fig. S3. Thermal ellipsoid diagram of the main molecular species in <i>rac</i> -3.	6
Fig. S4. EMAC-As ₂ (tartrate) ₂ interactions in 2 .	6
Fig. S5. Packing of <i>rac</i> -3.	7
Fig. S6. EMAC-As ₂ (tartrate) ₂ interactions in <i>rac</i> -3.	7
Fig. S7. Packing diagram along the <i>c</i> axis for 2 showing void spaces.	8
Fig. S8. Platon-generated thermal ellipsoid diagram of $[\Delta\text{-Co}_3(\text{dpa})_4\text{Cl}_2](\text{PF}_6)_2\cdot\text{MeCN}\cdot\text{C}_4\text{H}_{10}\text{O}$.	8
Fig. S9. End on view of the cation in $[\Delta\text{-Co}_3(\text{dpa})_4\text{Cl}_2](\text{PF}_6)_2\cdot\text{MeCN}\cdot\text{C}_4\text{H}_{10}\text{O}$.	9
Table S4. Crystal data and structure refinement for $[\Delta\text{-Co}_3(\text{dpa})_4\text{Cl}_2](\text{PF}_6)_2\cdot\text{MeCN}\cdot\text{C}_4\text{H}_{10}\text{O}$.	9
Fig. S10. Comparison of powder diffraction pattern of $\Delta\text{-2}$ (black) with those simulated from single crystal diffraction data for $\Delta\text{-2}$ (red) and <i>rac</i> -3 (blue).	10
Fig. S11. Comparison of powder diffraction pattern of the precipitate obtained when 0.5 eq of $\Delta\text{-1}$ was employed (black) and that simulated from single crystal diffraction data for $\Lambda\text{-2}$ (red) and <i>rac</i> -3 (blue).	10

Thermogravimetry

Fig. S12. Thermogravimetric analysis for $\Delta\text{-2}$.	11
--	----

Magnetism

Fig. S13. Field (left) and HT^{-1} (right) dependence of the magnetization.	12
---	----

X-ray absorption spectroscopy

Fig. S14. XMCD and $\text{XM}\chi\text{D}$ spectra for a sample of $\Delta\text{-2}$ at 17 T and 3.1 K.	13
Fig. S15. Angular dependence of XNCD as a function of angle θ .	13
Fig. S16. Comparison of XANES spectra with linearly and circularly polarized X-rays.	14

Circular Dichroism

Figure S17. Circular dichroism spectra in MeCN of $\Delta\text{-2}$ within 30 minutes of solution preparation and after 8 days of storage at room temperature.	15
Figure S18. Circular dichroism spectra in MeCN of $[\Delta\text{-Co}_3(\text{dpa})_4(\text{MeCN})_2](\text{PF}_6)_2$, as compared to $\Delta\text{-2}$; (left) freshly prepared $[\Delta\text{-Co}_3(\text{dpa})_4(\text{MeCN})_2](\text{PF}_6)_2$ solution; (right) after 5 days at r.t.	15

X-ray diffraction

Table S1. Bond lengths [\AA] and angles [$^\circ$] for $\Delta\text{-}2$.

C(1)-N(2)	1.361(3)	N(2)-C(1)-N(1)	115.2(2)	N(1)#1-Co(1)-N(4)#1	90.000(1)
C(1)-N(1)	1.373(3)	N(2)-C(1)-C(2)	120.6(2)	N(1)-Co(1)-N(4)#1	90.000(1)
C(1)-C(2)	1.410(3)	N(1)-C(1)-C(2)	124.0(2)	N(4)-Co(1)-N(4)#1	180.0
C(2)-C(3)	1.379(4)	C(3)-C(2)-C(1)	119.3(2)	N(1)#1-Co(1)-Co(2)#2	90.0
C(3)-C(4)	1.397(4)	C(2)-C(3)-C(4)	119.9(3)	N(1)-Co(1)-Co(2)#2	90.0
C(4)-C(5)	1.365(4)	C(5)-C(4)-C(3)	118.0(2)	N(4)-Co(1)-Co(2)#2	90.0
C(5)-N(2)	1.360(3)	N(2)-C(5)-C(4)	123.7(2)	N(4)#1-Co(1)-Co(2)#2	90.0
C(6)-N(3)	1.367(3)	N(3)-C(6)-N(4)#1	115.1(2)	N(1)#1-Co(1)-Co(2)	90.0
C(6)-N(4)#1	1.369(3)	N(3)-C(6)-C(7)	120.6(2)	N(1)-Co(1)-Co(2)	90.0
C(6)-C(7)	1.406(3)	N(4)#1-C(6)-C(7)	124.1(2)	N(4)-Co(1)-Co(2)	90.0
C(7)-C(8)	1.381(4)	C(8)-C(7)-C(6)	119.4(2)	N(4)#1-Co(1)-Co(2)	90.0
C(8)-C(9)	1.391(4)	C(7)-C(8)-C(9)	119.2(2)	Co(2)#2-Co(1)-Co(2)	180.0
C(9)-C(10)	1.352(4)	C(10)-C(9)-C(8)	119.0(2)	N(2)-Co(2)-Ni(2)#1	171.88(11)
C(10)-N(3)	1.356(3)	C(9)-C(10)-N(3)	123.7(2)	N(2)-Co(2)-Ni(3)#1	88.70(8)
C(11)-N(5)	1.136(5)	N(5)-C(11)-C(12)	180.0	N(2)#1-Co(2)-N(3)#1	90.67(8)
C(11)-C(12)	1.445(4)	O(3)-C(20)-O(2)	125.9(2)	N(2)-Co(2)-N(3)	90.67(8)
C(20)-O(3)	1.210(3)	O(3)-C(20)-C(21)	121.1(2)	N(2)#1-Co(2)-N(3)	88.70(8)
C(20)-O(2)	1.301(3)	O(2)-C(20)-C(21)	113.0(2)	N(3)#1-Co(2)-N(3)	171.19(11)
C(20)-C(21)	1.527(3)	O(1)-C(21)-C(20)	111.52(19)	N(2)-Co(2)-Ni(5)	94.06(6)
C(21)-O(1)	1.422(3)	O(1)-C(21)-C(22)	110.40(18)	N(2)#1-Co(2)-N(5)	94.06(6)
C(21)-C(22)	1.533(3)	C(20)-C(21)-C(22)	110.2(2)	N(3)#1-Co(2)-N(5)	94.41(6)
C(22)-O(4)	1.418(3)	O(4)-C(22)-C(23)	111.93(19)	N(3)-Co(2)-Ni(5)	94.41(6)
C(22)-C(23)	1.527(3)	O(4)-C(22)-C(21)	110.69(18)	N(2)-Co(2)-Co(1)	85.94(6)
C(23)-O(6)	1.218(3)	C(23)-C(22)-C(21)	108.46(18)	N(2)#1-Co(2)-Co(1)	85.94(6)
C(23)-O(5)	1.296(3)	O(6)-C(23)-O(5)	126.0(2)	N(3)#1-Co(2)-Co(1)	85.59(6)
C(100)-C(101)	1.492(5)	O(6)-C(23)-C(22)	120.6(2)	N(3)-Co(2)-Co(1)	85.59(6)
C(101)-C(102)	1.523(4)	O(5)-C(23)-C(22)	113.5(2)	N(5)-Co(2)-Co(1)	180.0
C(102)-C(103)	1.514(4)	C(100)-C(101)-C(102)	112.9(3)	O(4)#4-As(1)-O(1)	103.79(7)
C(103)-N(20)	1.511(3)	C(103)-C(102)-C(101)	111.1(2)	O(4)#4-As(1)-O(2)	85.80(7)
C(104)-C(105)	1.526(4)	N(20)-C(103)-C(102)	115.3(2)	O(1)-As(1)-O(2)	85.00(7)
C(104)-N(20)	1.529(3)	C(105)-C(104)-N(20)	114.9(2)	O(4)#4-As(1)-O(5)#4	83.93(7)
C(105)-C(106)	1.515(4)	C(106)-C(105)-C(104)	109.5(2)	O(1)-As(1)-O(5)#4	84.45(7)
C(106)-C(107)	1.539(4)	C(105)-C(106)-C(107)	110.5(2)	O(2)-As(1)-O(5)#4	163.09(7)
N(1)-C(1)#2	1.373(3)	C(1)-N(1)-C(1)#2	123.2(3)	N(1)#1-Co(1)-N(4)	90.0
N(1)-Co(1)	1.892(3)	C(1)-N(1)-Co(1)	118.41(14)	N(1)-Co(1)-N(4)	90.0
N(2)-Co(2)	1.987(2)	C(1)#2-N(1)-Co(1)	118.42(14)	N(1)#1-Co(1)-N(4)#1	90.000(1)
N(3)-Co(2)	1.988(2)	C(5)-N(2)-C(1)	118.4(2)	N(1)-Co(1)-N(4)#1	90.000(1)
N(4)-C(6)#2	1.369(3)	C(5)-N(2)-Co(2)	121.07(17)	N(4)-Co(1)-N(4)#1	180.0
N(4)-C(6)#1	1.369(3)	C(1)-N(2)-Co(2)	120.57(15)	N(1)#1-Co(1)-Co(2)#2	90.0
N(4)-Co(1)	1.893(3)	C(10)-N(3)-C(6)	118.1(2)	N(1)-Co(1)-Co(2)#2	90.0
N(5)-Co(2)	2.043(3)	C(10)-N(3)-Co(2)	121.32(16)	N(4)-Co(1)-Co(2)#2	90.0
N(20)-C(103)#3	1.511(3)	C(6)-N(3)-Co(2)	120.51(15)	N(4)#1-Co(1)-Co(2)#2	90.0
N(20)-C(104)#3	1.529(3)	C(6)#2-N(4)-C(6)#1	124.1(3)	N(1)#1-Co(1)-Co(2)	90.0
O(1)-As(1)	1.8017(16)	C(6)#2-N(4)-Co(1)	117.95(14)	N(1)-Co(1)-Co(2)	90.0
O(2)-As(1)	1.9888(17)	C(6)#1-N(4)-Co(1)	117.95(14)	N(4)-Co(1)-Co(2)	90.0
O(4)-As(1)#4	1.7966(16)	C(11)-N(5)-Co(2)	180.0	N(4)#1-Co(1)-Co(2)	90.0
O(5)-As(1)#4	2.0459(16)	C(103)-N(20)-C(103)#3	106.2(3)	Co(2)#2-Co(1)-Co(2)	180.0
Co(1)-N(1)#1	1.892(3)	C(103)-N(20)-C(104)	111.43(15)	N(2)-Co(2)-Ni(2)#1	171.88(11)
Co(1)-N(4)#1	1.894(3)	C(103)#3-N(20)-C(104)	111.29(15)	N(2)-Co(2)-Ni(3)#1	88.70(8)
Co(1)-Co(2)#2	2.3195(4)	C(103)-N(20)-C(104)#3	111.29(15)	N(2)#1-Co(2)-N(3)#1	90.67(8)
Co(1)-Co(2)	2.3196(4)	C(103)#3-N(20)-C(104)#3	111.43(15)	N(2)-Co(2)-N(3)	90.67(8)
Co(2)-N(2)#1	1.987(2)	C(104)-N(20)-C(104)#3	105.3(3)	N(2)#1-Co(2)-N(3)	88.70(8)
Co(2)-N(3)#1	1.988(2)	C(21)-O(1)-As(1)	116.07(13)	N(3)#1-Co(2)-N(3)	171.19(11)
As(1)-O(4)#4	1.7966(16)	C(20)-O(2)-As(1)	114.06(15)	N(2)-Co(2)-Ni(5)	94.06(6)
As(1)-O(5)#4	2.0459(16)	C(22)-O(4)-As(1)#4	116.95(13)	N(2)#1-Co(2)-N(5)	94.06(6)
		C(23)-O(5)-As(1)#4	112.62(14)	N(3)#1-Co(2)-N(5)	94.41(6)
		N(1)#1-Co(1)-N(1)	180.0	N(3)-Co(2)-Ni(5)	94.41(6)
		N(1)#1-Co(1)-N(4)	90.0	N(2)-Co(2)-Co(1)	85.94(6)
		N(1)-Co(1)-N(4)	90.0	N(2)#1-Co(2)-Co(1)	85.94(6)

Symmetry transformations used to generate equivalent atoms: #1 -x+1,-y+1,z; #2 y,x,-z; #3 -y+1,-x+1,-z+1; #4 y,x,-z+1

Table S2. Bond lengths [Å] and angles [°] for Λ-2.

C(1)-N(2)	1.359(4)	N(2)-C(1)-N(1)	115.1(3)	C(10)#1-N(3)-Co2	121.5(2)
C(1)-N(1)	1.377(4)	N(2)-C(1)-C(2)	120.3(3)	C(107)-C(106)-C(105)	110.3(4)
C(1)-C(2)	1.409(5)	N(1)-C(1)-C(2)	124.4(3)	C(1)-N(1)-C(1)#3	123.2(4)
C(2)-C(3)	1.361(6)	C(3)-C(2)-C(1)	120.4(4)	C(1)-N(1)-Co1	118.4(2)
C(3)-C(4)	1.399(6)	C(2)-C(3)-C(4)	119.1(4)	C(1)#3-N(1)-Co1	118.4(2)
C(4)-C(5)	1.368(6)	C(5)-C(4)-C(3)	118.3(3)	C(5)-N(2)-C(1)	118.1(3)
C(5)-N(2)	1.356(4)	N(2)-C(5)-C(4)	123.6(3)	C(5)-N(2)-Co2	121.3(2)
C(6)-N(3)#1	1.358(4)	N(3)#1-C(6)-N(4)	115.3(3)	C(1)-N(2)-Co2	120.6(2)
C(6)-N(4)	1.372(4)	N(3)#1-C(6)-C(7)	120.4(3)	C(10)#1-N(3)-C(6)#1	117.8(3)
C(6)-C(7)	1.408(5)	N(4)-C(6)-C(7)	124.0(3)	C(10)#1-N(3)-Co2	121.5(2)
C(7)-C(8)	1.363(6)	C(8)-C(7)-C(6)	120.4(3)	C(107)-C(106)-C(105)	110.3(4)
C(8)-C(9)	1.402(6)	C(7)-C(8)-C(9)	118.6(4)	C(6)#1-N(3)-Co2	120.7(2)
C(9)-C(10)	1.349(6)	C(10)-C(9)-C(8)	118.8(4)	C(6)-N(4)-C(6)#4	124.7(4)
C(10)-N(3)#1	1.354(4)	C(9)-C(10)-N(3)#1	124.0(3)	C(6)-N(4)-Co1	117.7(2)
C(11)-N(5)	1.152(6)	N(5)-C(11)-C(12)	180.0	C(6)#4-N(4)-Co1	117.7(2)
C(11)-C(12)	1.453(6)	O(3)-C(20)-O(2)	124.5(3)	C(11)-N(5)-Co2	180.0
C(20)-O(3)	1.228(5)	O(3)-C(20)-C(21)	121.7(4)	C(103)-N(20)-C(103)#5	106.9(4)
C(20)-O(2)	1.306(5)	O(2)-C(20)-C(21)	113.7(3)	C(103)-N(20)-C(104)#5	111.2(2)
C(20)-C(21)	1.508(5)	N(2)-C(1)-N(1)	115.1(3)	C(103)#5-N(20)-C(104)#5	111.4(2)
C(21)-O(1)	1.418(4)	N(2)-C(1)-C(2)	120.3(3)	C(103)-N(20)-C(104)	111.4(2)
C(21)-C(22)	1.528(5)	N(1)-C(1)-C(2)	124.4(3)	C(103)#5-N(20)-C(104)	111.2(2)
C(22)-O(4)#2	1.412(4)	C(3)-C(2)-C(1)	120.4(4)	C(104)#5-N(20)-C(104)	104.9(4)
C(22)-C(23)	1.517(5)	C(2)-C(3)-C(4)	119.1(4)	N(1)#1-Co1-N(4)	90.0
C(23)-O(6)	1.224(4)	C(5)-C(4)-C(3)	118.3(3)	N(1)-Co1-N(4)	90.0
C(23)-O(5)#2	1.297(4)	N(2)-C(5)-C(4)	123.6(3)	N(1)#1-Co1-N(4)#1	90.0
C(100)-C(101)	1.485(8)	N(3)#1-C(6)-N(4)	115.3(3)	N(1)-Co1-N(4)#1	90.0
C(101)-C(102)	1.539(7)	N(3)#1-C(6)-C(7)	120.4(3)	N(4)-Co1-N(4)#1	180.0
C(102)-C(103)	1.506(7)	N(4)-C(6)-C(7)	124.0(3)	N(1)#1-Co1-Co2#3	90.0
C(103)-N(20)	1.526(5)	C(8)-C(7)-C(6)	120.4(3)	N(1)-Co1-Co2#3	90.0
C(104)-N(20)	1.530(4)	C(7)-C(8)-C(9)	118.6(4)	N(4)-Co1-Co2#3	90.0
C(104)-C(105)	1.527(6)	C(10)-C(9)-C(8)	118.8(4)	N(4)#1-Co1-Co2#3	90.0
C(105)-C(106)	1.531(6)	C(9)-C(10)-N(3)#1	124.0(3)	N(1)#1-Co1-Co2	90.0
C(106)-C(107)	1.526(7)	N(5)-C(11)-C(12)	180.0	N(1)-Co1-Co2	90.0
N(1)-C(1)#3	1.377(4)	O(1)-C(21)-C(20)	111.9(3)	N(4)-Co1-Co2	90.0
N(1)-Co1	1.888(4)	O(1)-C(21)-C(22)	110.5(3)	N(4)#1-Co1-Co2	90.0
N(2)-Co2	1.983(3)	C(20)-C(21)-C(22)	110.6(3)	Co2#3-Co1-Co2	180.0
N(3)-C(10)#1	1.354(4)	O(4)#2-C(22)-C(23)	111.8(3)	N(3)-Co2-N(3)#1	171.22(16)
N(3)-C(6)#1	1.358(4)	O(4)#2-C(22)-C(21)	110.6(3)	N(3)-Co2-N(2)#1	88.83(11)
N(3)-Co2	1.982(3)	C(23)-C(22)-C(21)	108.5(3)	N(3)#1-Co2-N(2)#1	90.55(11)
N(4)-C(6)#4	1.372(4)	O(6)-C(23)-O(5)#2	124.7(3)	N(3)-Co2-N(2)	90.55(11)
N(4)-Co1	1.895(4)	O(6)-C(23)-C(22)	121.2(3)	N(3)#1-Co2-N(2)	88.84(11)
N(5)-Co2	2.022(4)	O(5)#2-C(23)-C(22)	114.2(3)	N(2)#1-Co2-N(2)	172.00(16)
N(20)-C(103)#5	1.527(5)	C(100)-C(101)-C(102)	111.2(4)	N(3)-Co2-N(5)	94.39(8)
N(20)-C(104)#5	1.530(4)	C(103)-C(102)-C(101)	109.1(4)	N(3)#1-Co2-N(5)	94.39(8)
O(1)-As1	1.803(2)	C(102)-C(103)-N(20)	114.8(3)	N(2)#1-Co2-N(5)	94.00(8)
O(2)-As1	1.993(3)	N(20)-C(104)-C(105)	114.2(3)	N(2)-Co2-N(5)	94.00(8)
O(4)-C(22)#2	1.412(4)	C(106)-C(105)-C(104)	109.4(3)	N(3)-Co2-Co1	85.61(8)
O(4)-As1	1.794(2)	C(107)-C(106)-C(105)	110.3(4)	N(3)#1-Co2-Co1	85.61(8)
O(5)-C(23)#2	1.297(4)	C(1)-N(1)-C(1)#3	123.2(4)	N(2)#1-Co2-Co1	86.00(8)
O(5)-As1	2.046(2)	C(1)-N(1)-Co1	118.4(2)	N(2)-Co2-Co1	86.00(8)
Co1-N(1)#1	1.888(4)	C(1)#3-N(1)-Co1	118.4(2)	N(5)-Co2-Co1	180.0
Co1-N(4)#1	1.895(4)	C(5)-N(2)-C(1)	118.1(3)	O(4)-As1-O(1)	103.76(11)
Co1-Co2#3	2.3160(6)	C(5)-N(2)-Co2	121.3(2)	O(4)-As1-O(2)	85.73(11)
Co1-Co2	2.3160(6)	C(1)-N(2)-Co2	120.6(2)	O(1)-As1-O(2)	85.07(10)
Co2-N(3)#1	1.982(3)	C(10)#1-N(3)-C(6)#1	117.8(3)	O(4)-As1-O(5)	84.04(10)
Co2-N(2)#1	1.983(3)	C(21)-O(1)-As1	115.79(19)	O(1)-As1-O(5)	84.41(10)
		C(20)-O(2)-As1	113.1(2)	O(2)-As1-O(5)	163.15(10)
		C(22)#2-O(4)-As1	117.1(2)	N(3)-Co2-Co1	85.61(8)
		C(23)#2-O(5)-As1	112.0(2)	N(3)#1-Co2-Co1	85.61(8)
		N(1)#1-Co1-N(1)	180.00(12)		

Symmetry transformations used to generate equivalent atoms: #1 -x+1,-y+1,z; #2 y,x,-z+1; #3 y,x,-z+2; #4 -y+1,-x+1,-z+2; #5 -y+1,-x+1,-z+1

Table S3. Bond lengths [Å] and angles [°] for *rac*-3.

C(1)-N(1)	1.351(2)	N(1)-C(1)-C(2)	123.58(18)	N(6)-Co(1)-N(1)	89.41(6)
C(1)-C(2)	1.380(3)	C(1)-C(2)-C(3)	118.46(18)	N(4)-Co(1)-N(8)	94.98(6)
C(2)-C(3)	1.390(3)	C(4)-C(3)-C(2)	119.41(18)	N(3)-Co(1)-N(8)	92.56(7)
C(3)-C(4)	1.377(3)	C(3)-C(4)-C(5)	119.67(18)	N(6)-Co(1)-N(8)	96.60(7)
C(4)-C(5)	1.407(3)	N(2)-C(5)-N(1)	114.72(16)	N(1)-Co(1)-N(8)	93.89(6)
C(5)-N(2)	1.367(2)	N(2)-C(5)-C(4)	124.09(17)	N(4)-Co(1)-Co(2)	87.33(5)
C(5)-N(1)	1.368(2)	N(1)-C(5)-C(4)	120.89(16)	N(3)-Co(1)-Co(2)	85.04(5)
C(6)-N(3)	1.354(2)	N(3)-C(6)-C(7)	123.64(18)	N(3)-Co(1)-N(1)	90.75(6)
C(6)-C(7)	1.374(3)	C(6)-C(7)-C(20)#1	118.13(18)	N(1)-Co(1)-Co(2)	83.84(5)
C(7)-C(20)#1	1.390(3)	N(4)-C(8)-C(9)	122.88(18)	N(8)-Co(1)-Co(2)	176.67(5)
C(8)-N(4)	1.357(2)	C(8)-C(9)-C(10)	118.57(18)	N(2)-Co(2)-N(7)#1	89.25(5)
C(8)-C(9)	1.376(3)	C(11)-C(10)-C(9)	119.53(18)	N(2)-Co(2)-N(7)	89.25(5)
C(9)-C(10)	1.398(3)	C(10)-C(11)-C(12)	119.94(18)	N(7)#1-Co(2)-N(7)	178.51(9)
C(10)-C(11)	1.371(3)	N(5)-C(12)-N(4)	115.32(16)	N(2)-Co(2)-N(5)	180.0
C(11)-C(12)	1.413(3)	N(5)-C(12)-C(11)	124.26(17)	N(7)#1-Co(2)-N(5)	90.75(5)
C(12)-N(5)	1.363(2)	N(4)-C(12)-C(11)	120.15(16)	N(7)-Co(2)-N(5)	90.75(5)
C(12)-N(4)	1.366(2)	N(6)-C(13)-C(14)	123.42(19)	N(2)-Co(2)-Co(1)	92.004(10)
C(13)-N(6)	1.354(2)	C(13)-C(14)-C(15)	118.63(19)	N(7)#1-Co(2)-Co(1)	89.74(5)
C(13)-C(14)	1.372(3)	C(16)-C(15)-C(14)	119.00(19)	N(7)-Co(2)-Co(1)	90.31(5)
C(14)-C(15)	1.394(3)	C(15)-C(16)-C(17)	120.44(19)	N(5)-Co(2)-Co(1)	87.996(10)
C(15)-C(16)	1.374(3)	N(6)-C(17)-N(7)	115.45(16)	N(2)-Co(2)-Co(1)#1	92.003(10)
C(16)-C(17)	1.413(3)	N(6)-C(17)-C(16)	119.74(17)	N(7)#1-Co(2)-Co(1)#1	90.31(5)
C(17)-N(6)	1.366(2)	N(7)-C(17)-C(16)	124.69(17)	N(7)-Co(2)-Co(1)#1	89.74(5)
C(17)-N(7)	1.367(2)	N(3)#1-C(18)-N(7)	114.99(16)	N(5)-Co(2)-Co(1)#1	87.997(10)
C(18)-N(3)#1	1.362(2)	N(3)#1-C(18)-C(19)	119.86(17)	Co(1)-Co(2)-Co(1)#1	175.99(2)
C(18)-N(7)	1.364(2)	N(7)-C(18)-C(19)	124.85(17)	C(1)-N(1)-C(5)	117.92(16)
C(18)-C(19)	1.416(3)	C(20)-C(19)-C(18)	119.80(18)	C(1)-N(1)-Co(1)	120.85(13)
C(19)-C(20)	1.377(3)	C(19)-C(20)-C(7)#1	119.60(18)	C(5)-N(1)-Co(1)	121.19(12)
C(20)-C(7)#1	1.390(3)	N(8)-C(21)-C(22)	178.8(2)	C(5)#1-N(2)-C(5)	124.7(2)
C(21)-N(8)	1.145(3)	O(5)-C(100)-O(1)	125.17(19)	C(5)#1-N(2)-Co(2)	117.65(11)
C(21)-C(22)	1.450(3)	O(5)-C(100)-C(101)	120.96(19)	C(5)-N(2)-Co(2)	117.65(11)
C(100)-O(5)	1.222(3)	O(1)-C(100)-C(101)	113.87(17)	C(6)-N(3)-C(18)#1	118.56(16)
C(100)-O(1)	1.296(3)	O(2)-C(101)-C(100)	111.41(16)	C(6)-N(3)-Co(1)	121.00(13)
C(100)-C(101)	1.518(3)	O(2)-C(101)-C(101)#2	109.65(13)	C(18)#1-N(3)-Co(1)	120.35(12)
C(101)-O(2)	1.419(2)	C(100)-C(101)-C(101)#2	108.84(19)	C(8)-N(4)-C(12)	118.91(16)
C(101)-C(101)#2	1.521(4)	O(4)-C(102)-C(102)#2	110.37(14)	C(8)-N(4)-Co(1)	121.94(13)
C(102)-O(4)	1.411(2)	O(4)-C(102)-C(103)	111.92(16)	C(12)-N(4)-Co(1)	119.00(12)
C(102)-C(102)#2	1.519(4)	C(102)#2-C(102)-C(103)	109.8(2)	C(12)-N(5)-C(12)#1	122.9(2)
C(102)-C(103)	1.533(3)	O(6)-C(103)-O(3)	125.80(19)	C(12)-N(5)-Co(2)	118.55(11)
C(103)-O(6)	1.225(3)	O(6)-C(103)-C(102)	120.36(19)	C(12)#1-N(5)-Co(2)	118.55(11)
C(103)-O(3)	1.296(3)	O(3)-C(103)-C(102)	113.84(18)	C(13)-N(6)-C(17)	118.68(16)
C(200)-N(200)	1.137(3)	N(200)-C(200)-C(201)	179.9(3)	C(13)-N(6)-Co(1)	120.61(13)
C(200)-C(201)	1.451(3)	O(2)-As(1)-O(4)	102.56(6)	C(17)-N(6)-Co(1)	120.68(12)
As(1)-O(2)	1.7960(14)	O(2)-As(1)-O(1)	84.94(6)	C(18)-N(7)-C(17)	124.68(16)
As(1)-O(4)	1.8008(14)	O(4)-As(1)-O(1)	83.75(6)	C(18)-N(7)-Co(2)	118.11(12)
As(1)-O(1)	1.9954(15)	O(2)-As(1)-O(3)	84.34(6)	C(17)-N(7)-Co(2)	117.13(12)
As(1)-O(3)	2.0574(16)	O(4)-As(1)-O(3)	83.92(6)	C(21)-N(8)-Co(1)	166.99(16)
Co(1)-N(4)	1.9662(16)	O(1)-As(1)-O(3)	161.50(6)	C(100)-O(1)-As(1)	113.28(12)
Co(1)-N(3)	1.9770(16)	N(4)-Co(1)-N(3)	89.51(6)	C(101)-O(2)-As(1)	116.22(11)
Co(1)-N(6)	1.9780(16)	N(4)-Co(1)-N(6)	88.93(6)	C(103)-O(3)-As(1)	112.70(13)
Co(1)-N(1)	2.0108(16)	N(3)-Co(1)-N(6)	170.81(7)	C(102)-O(4)-As(1)	117.61(11)
Co(1)-N(8)	2.0731(18)	N(4)-Co(1)-N(1)	171.11(6)		
Co(1)-Co(2)	2.3111(7)				
Co(2)-N(2)	1.866(2)				
Co(2)-N(7)#1	1.9000(15)				
Co(2)-N(7)	1.9000(15)				

Symmetry transformations used to generate equivalent atoms: #1 -x+1,y,-z+1/2; #2 -x,y,-z+1/2

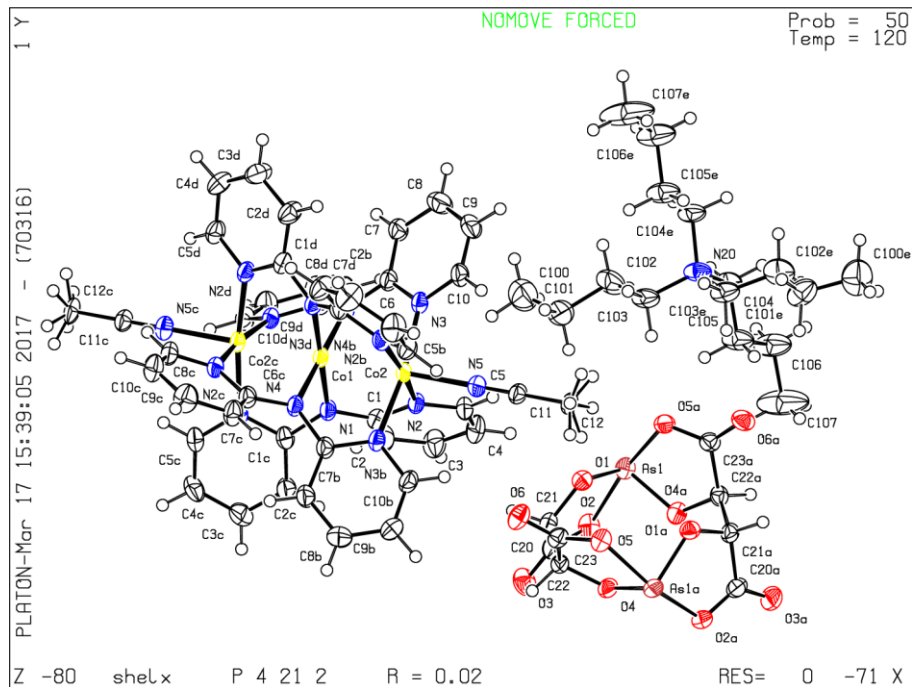


Fig. S1. Platon-generated thermal ellipsoid diagram of the main molecular species in $\Delta\text{-}2$.

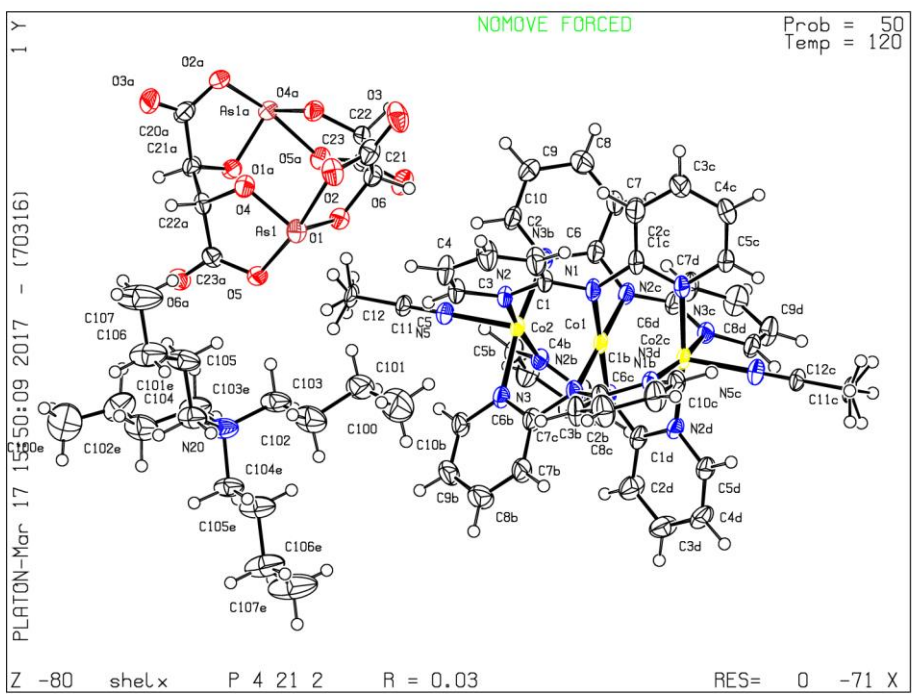


Fig. S2. Platon-generated thermal ellipsoid diagram of the main molecular species in $\Lambda\text{-}2$.

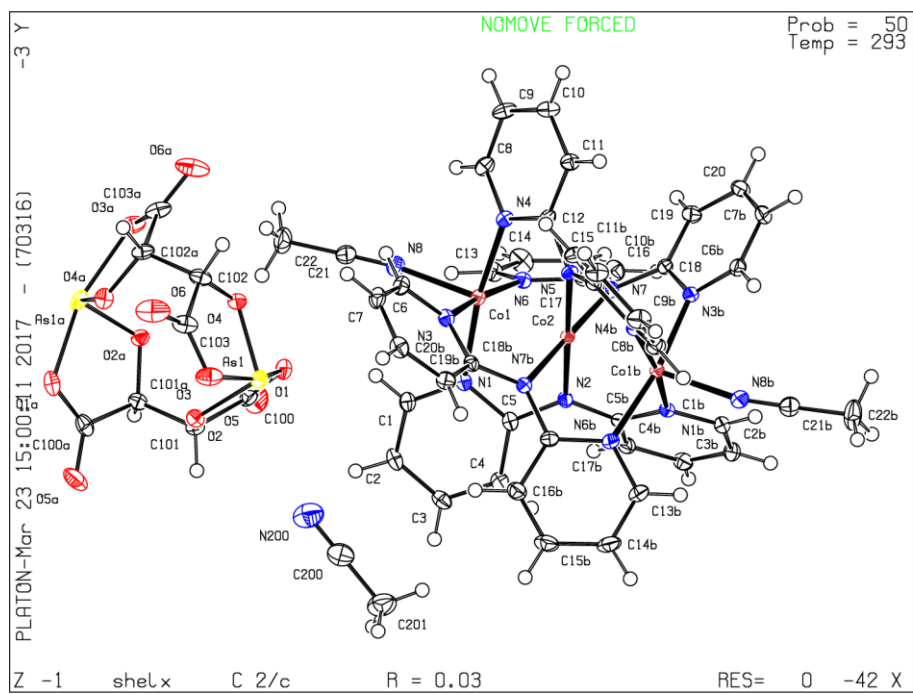


Fig. S3. Platon-generated thermal ellipsoid diagram of the main molecular species in *rac*-3.

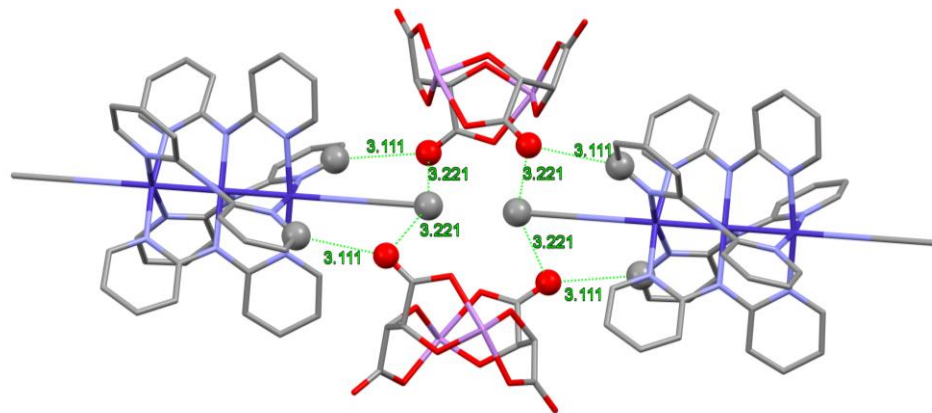


Fig. S4 EMAC- $\text{As}_2(\text{tartrate})_2$ interactions in 2.

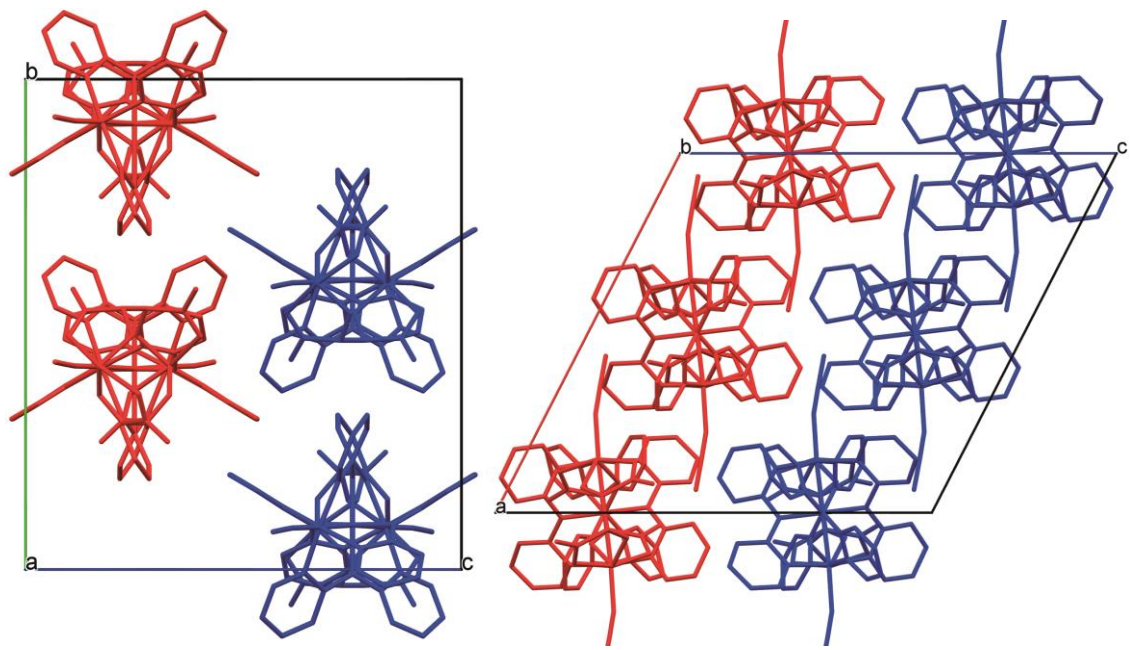


Fig. S5. Packing of *rac*-3 viewed along the *a* axis (left) and along the *b* axis (right). The different handedness of the compounds are demonstrated by different colors. Anions and solvents omitted.

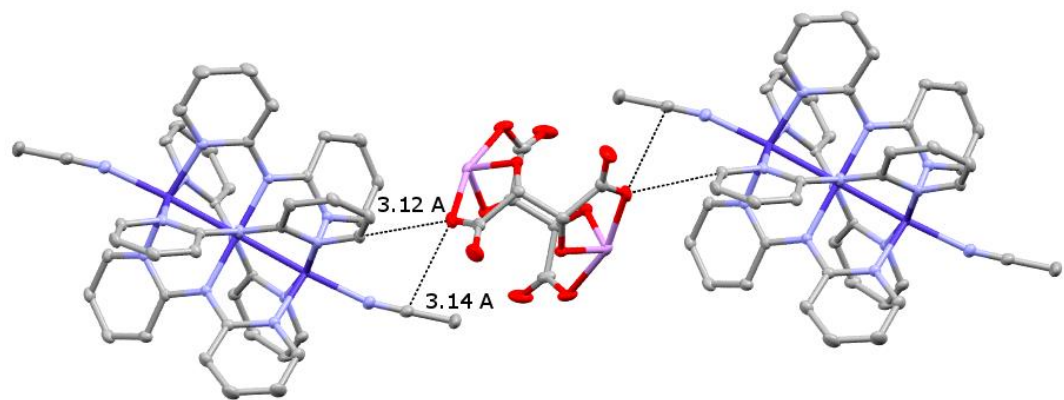


Fig. S6. EMAC- $\text{As}_2(\text{tartrate})_2$ interactions in *rac*-3.

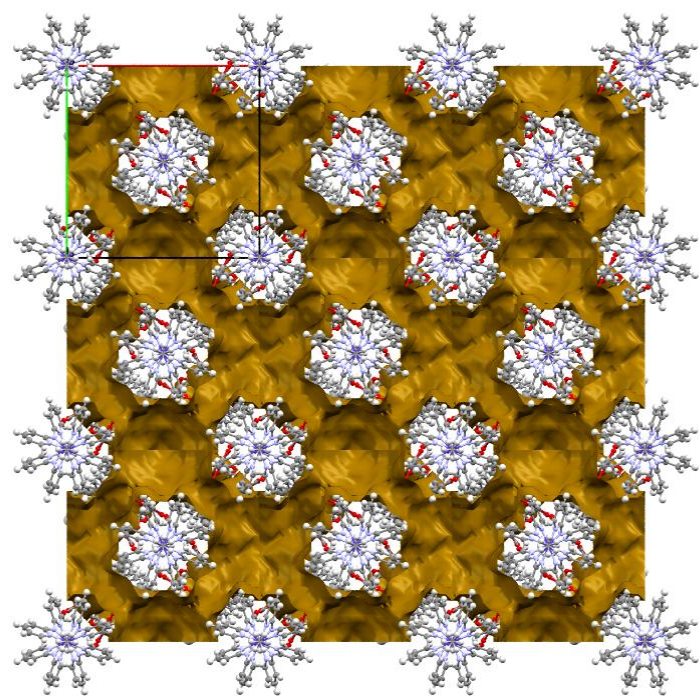


Fig. S7. Packing diagram along the *c* axis showing void spaces calculated by Mercury with a 1.2 Å probe radius.

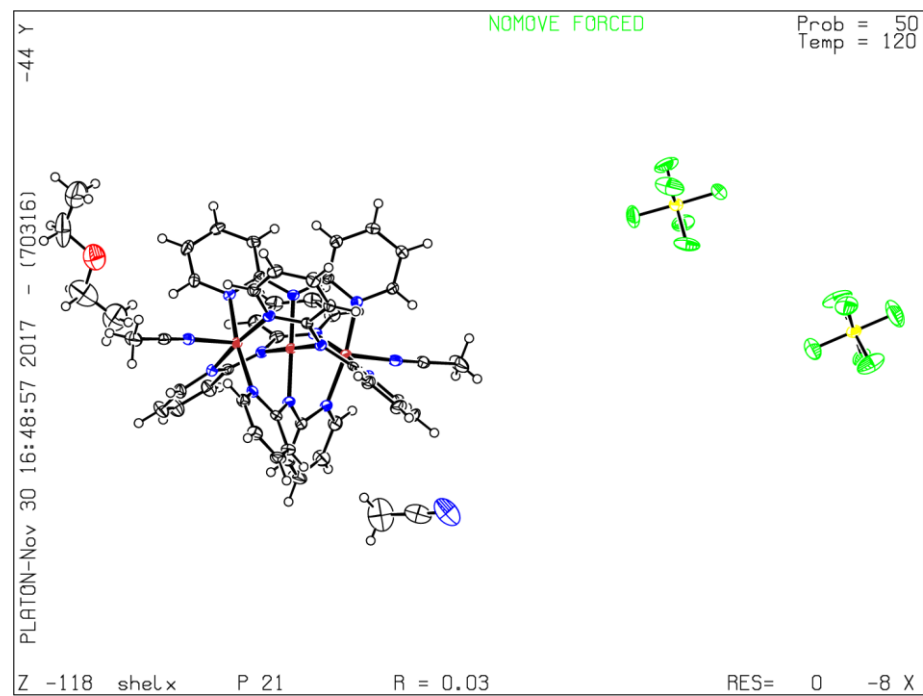


Fig. S8. Platon-generated thermal ellipsoid diagram of $[\Delta\text{-Co}_3(\text{dpa})_4\text{Cl}_2](\text{PF}_6)_2 \cdot \text{MeCN} \cdot \text{C}_4\text{H}_{10}\text{O}$.

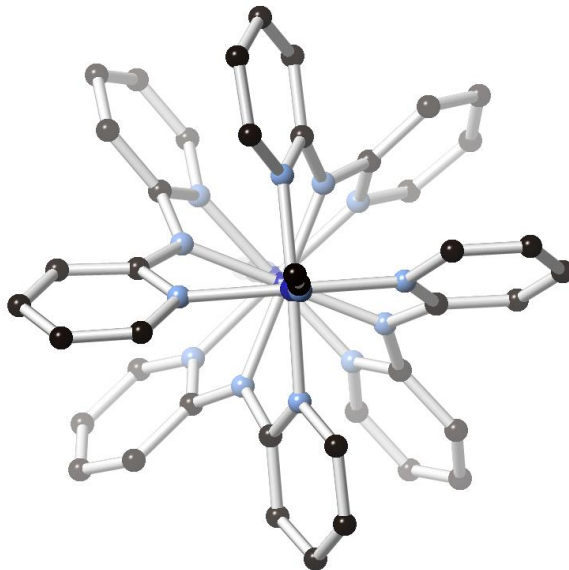


Fig. S9. End on view of the cation in $[\Delta\text{-Co}_3(\text{dpa})_4\text{Cl}_2](\text{PF}_6)_2 \cdot \text{MeCN} \cdot \text{C}_4\text{H}_{10}\text{O}$ showing the clockwise wrapping of the dipyridylamine ligand.

Table S4. Crystal data and structure refinement for $[\Delta\text{-Co}_3(\text{dpa})_4\text{Cl}_2](\text{PF}_6)_2 \cdot \text{MeCN} \cdot \text{C}_4\text{H}_{10}\text{O}$

Empirical formula	C50 H51 Co3 F12 N15 O P2
Formula weight / g.mol ⁻¹	1344.78
Temperature / K	120(2)
Wavelength / Å	0.71073
Space group	<i>P</i> 2 ₁
Unit cell dimensions	
<i>a</i> /Å	11.7226(9)
<i>b</i> /Å	21.8073(17)
<i>c</i> /Å	12.0149(9)
β°	112.115(3)
Volume / Å ³	2845.5(4)
Z, Calculated density / Mg/m ³	2, 1.570
Absorption coefficient / mm ⁻¹	1.012
<i>F</i> (000)	1366
Crystal size / mm	0.34 × 0.23 × 0.04
Orientation reflections: number, range (θ)	9958, 2.27-25.33°
θ range for data collection / °	1.83-25.39
Limiting indices	-14 ≤ <i>h</i> ≤ 14, -26 ≤ <i>k</i> ≤ 26, -14 ≤ <i>l</i> ≤ 14
Reflections collected / unique	10437 / 9989 [<i>R</i> (int) = 0.0404]
Completeness to $\theta = 25.33$	99.80%
Scan method	ϕ and ω scans
Absorption correction	Semi-empirical
Max. and min. transmission	0.7452 and 6624
Refinement method	Full-matrix least-squares on <i>F</i> ²
Data / parameters / restraints	10437 / 751 / 1
Goodness-of-fit on <i>F</i> ²	1.070
Final <i>R</i> indices [<i>I</i> > 2σ(<i>I</i>)]	<i>R</i> ₁ ^a = 0.0303, <i>wR</i> ₂ ^b = 0.0807
<i>R</i> indices (all data)	<i>R</i> ₁ ^a = 0.0327, <i>wR</i> ₂ ^b = 0.0821
Flack parameter	0.002(3)

^a $R_1 = \sum \|F_o - |F_c|\| / \sum |F_o|$.

^b $wR_2 = [\sum [w(F_o^2 - F_c^2)^2] / \sum [w(F_o^2)^2]]^{1/2}$, $w = 1/\sigma^2(F_o^2) + (aP)^2 + bP$, where $P = [\max(0 \text{ or } F_o^2) + 2(F_c^2)]/3$.

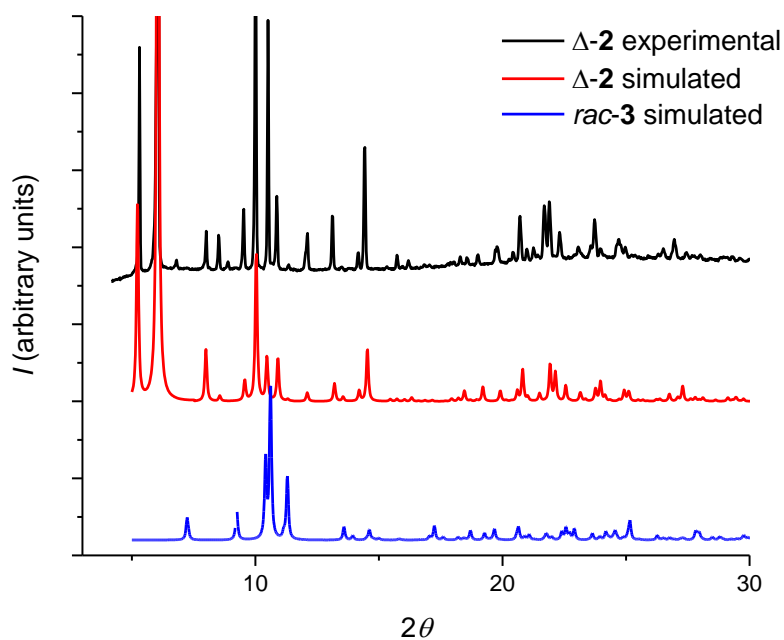


Fig. S10. Comparison of powder diffraction pattern of $\Delta\text{-}2$ (black) with those simulated from single crystal diffraction data for $\Delta\text{-}2$ (red) and $rac\text{-}3$ (blue).

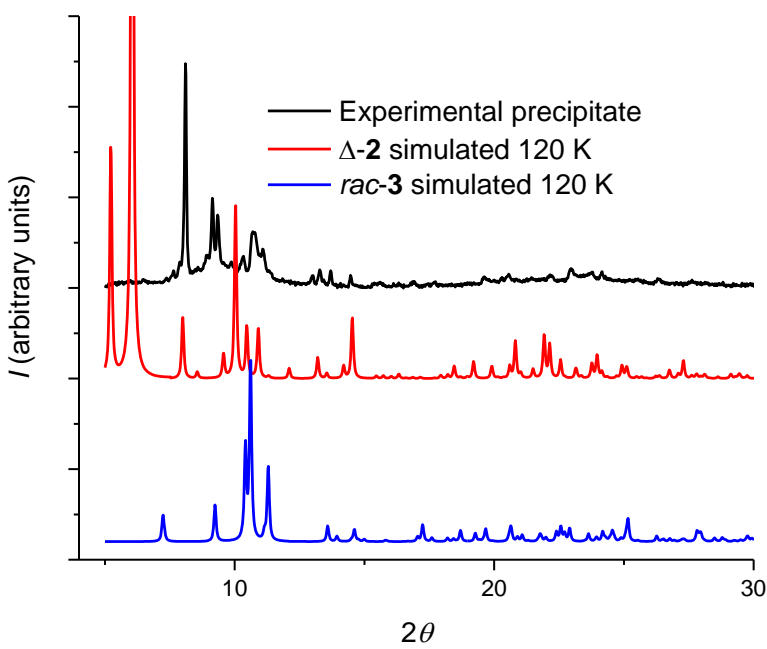


Fig. S11. Comparison of powder diffraction pattern of the precipitate obtained when 0.5 eq of $\Delta\text{-}1$ was employed (black) and that simulated from single crystal diffraction data for $\Delta\text{-}2$ (red) and $rac\text{-}3$ (blue).

Thermogravimetry

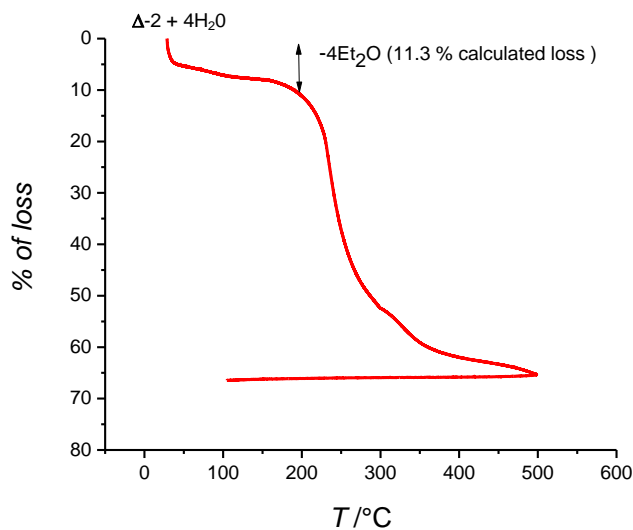


Fig. S12. Thermogravimetric analysis for $\Delta\text{-}2$ with a heating ramp of $2^\circ\text{C}/\text{min}$ to 300°C and then $5^\circ\text{C}/\text{min}$ to 500°C

Magnetism

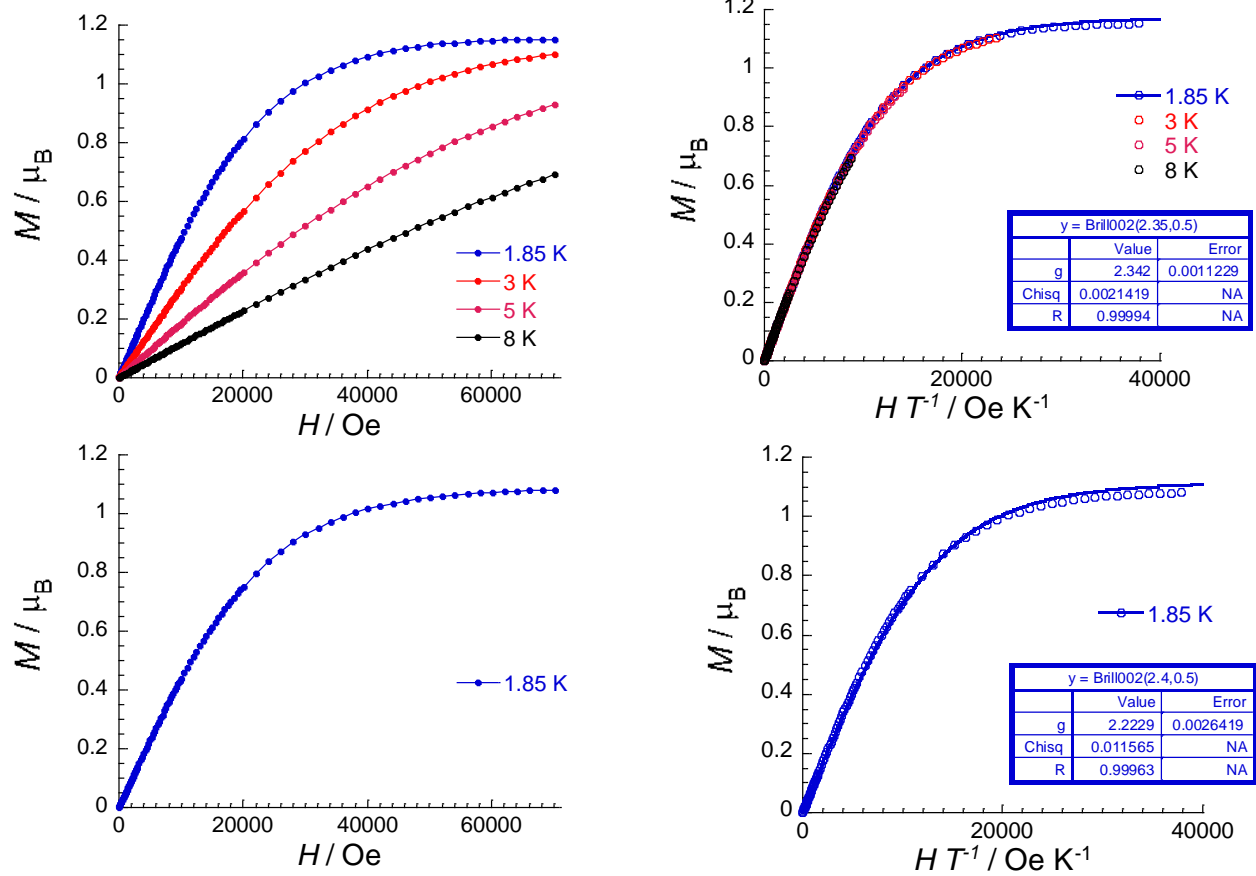


Fig. S13. Field (left) and HT^{-1} (right) dependence of the magnetization for $\Delta\text{-}2$ (top) and $\Lambda\text{-}2$ (bottom).

X-ray absorption spectroscopy

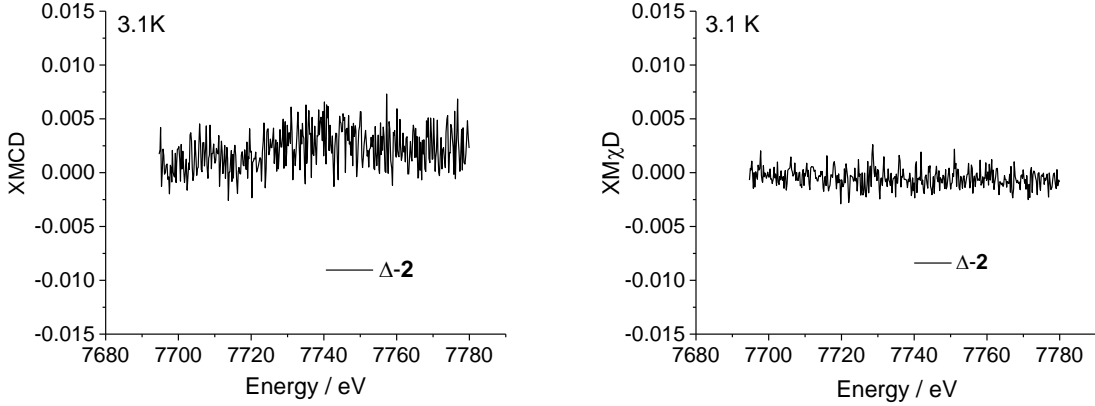


Fig. S14. (left) XMCD spectrum of $\Delta\text{-}2$ at ± 17 T and 3.1 K calculated according to Eq. 1 in the text; (right) XM χ D spectrum of $\Delta\text{-}2$ at ± 17 T and 3.1 K calculated according to Eq. 2 in the text.

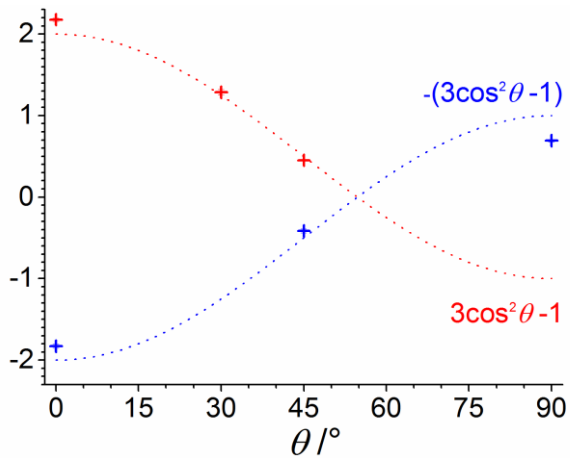


Fig. S15. Angular dependence of XNCD for $\Delta\text{-}2$ (red) and $\Lambda\text{-}2$ (blue). As a reference for linear interpolation for all other spectra, we chose the spectral shape obtained by calculating the half-difference of the XNCD spectra of $\Delta\text{-}2$ and $\Lambda\text{-}2$ at $\theta = 0$, calculated as described in the text. Dotted lines are eye-guides for the $\pm (3\cos^2\theta - 1)$ functions. The values obtained through those fits were multiplied by 2 then plotted as a function of θ .

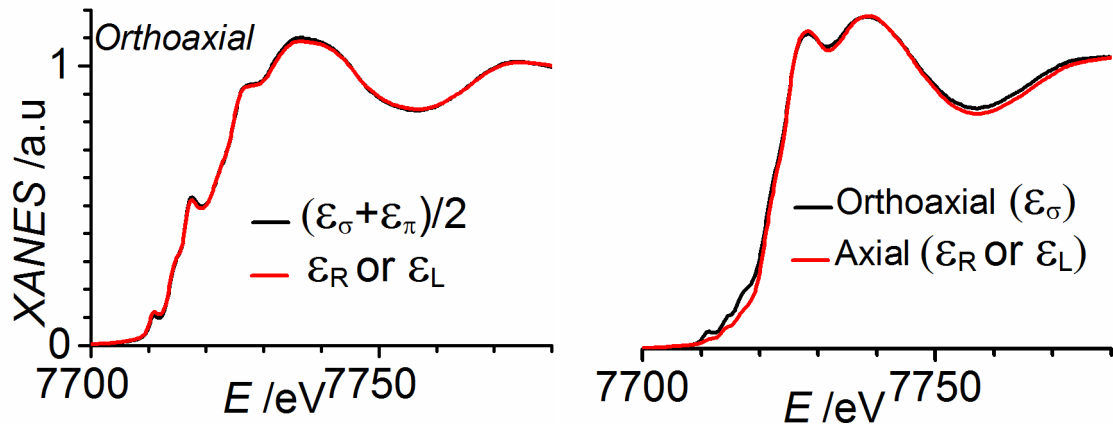


Fig. S16. (left) Superposition of XANES spectra for $\theta = 90^\circ$ obtained with circularly polarized X-rays and the average of the spectra obtained from horizontally and vertically polarized X-rays; (right) Superposition of XANES spectra obtained with circularly polarized X-rays for $\theta = 0^\circ$ and with horizontally polarized X-rays for $\theta = 90^\circ$. The observed difference in the pre-edge features is due to a not-identical alignment of the X-ray wavevector with respect to the *c*-axis of the crystals in the two experiments.

Circular dichroism spectroscopy

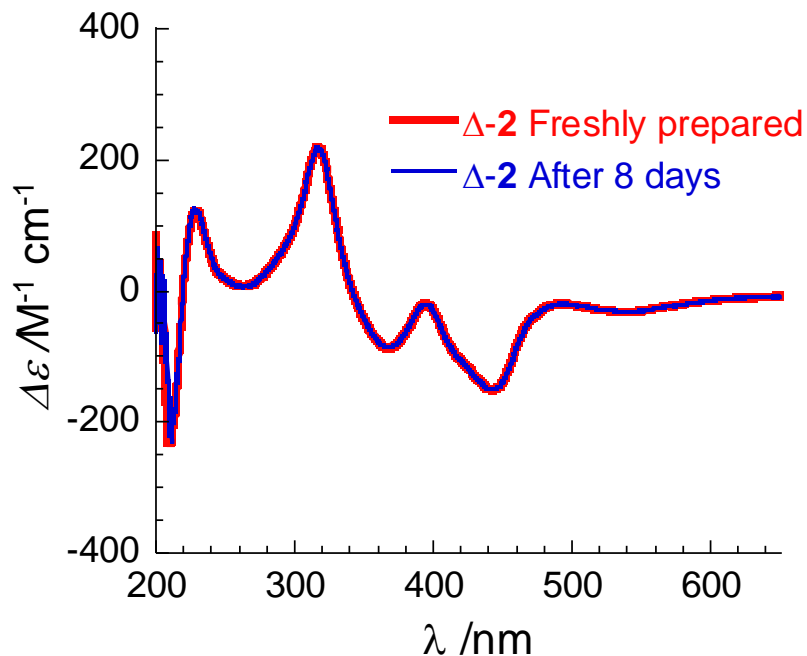


Figure S17. Circular dichroism spectra in MeCN of $\Delta\text{-2}$ within 30 minutes of solution preparation and after 8 days of storage at room temperature.

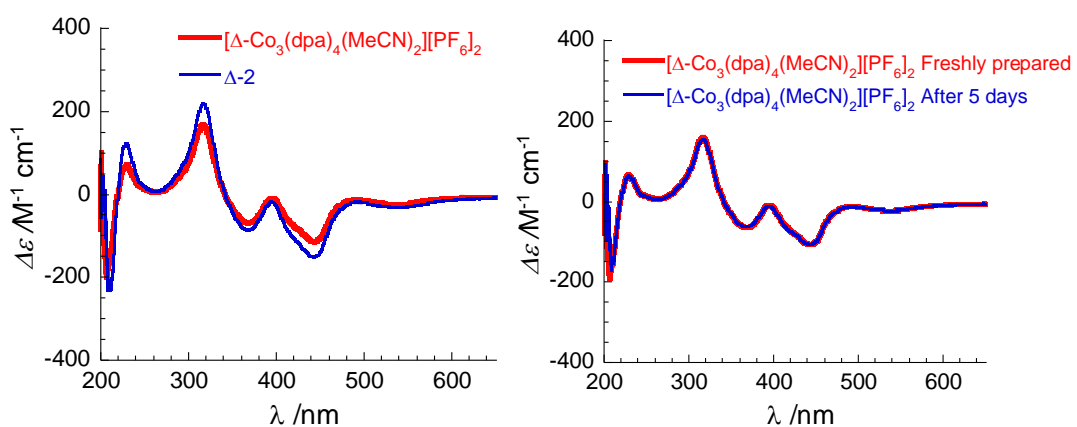


Figure S18. Circular dichroism spectra in MeCN of $[\Delta\text{-Co}_3(\text{dpa})_4(\text{MeCN})_2]\text{[PF}_6\text{]}_2$ obtained by an anion-exchange reaction and subsequent recrystallization from acetonitrile and diethyl ether, as compared to $\Delta\text{-2}$; (left) freshly prepared $[\Delta\text{-Co}_3(\text{dpa})_4(\text{MeCN})_2]\text{[PF}_6\text{]}_2$ solution; (right) after 5 days at r.t.